This full text paper was peer reviewed at the direction of IEEE Communications Society subject matter experts for publication in the IEEE DySPAN 2010 proceedings

A 50MHz-to-1.5GHz Cross-Correlation CMOS Spectrum Analyzer for Cognitive Radio with 89dB SFDR in 1MHz RBW

Mark S. Oude Alink, Eric A.M. Klumperink, Michiel C.M. Soer, André B.J. Kokkeler and Bram Nauta
Integrated Circuit Design / Computer Architecture for Embedded Systems
CTIT Research Institute, University of Twente, Enschede, The Netherlands
Email: m.s.oudealink@utwente.nl

***Abstract*—Spectrum sensing for cognitive radio requires a high linearity to handle strong signals, and at the same time a low noise figure (NF) to enable detection of much weaker signals. Often there is a trade-off between linearity and noise: improving one of them degrades the other. Cross-correlation can break this trade-off by reducing noise at the cost of measurement time. An existing RF front-end in CMOS-technology with IIP3=+11dBm and NF<6.5dB is duplicated and attenuators are put in front to increase linearity (IIP3=+24dBm). The attenuation degrades NF, but by using cross-correlation of the outputs of the two front-ends, the NF is reduced to below 4dB. In total this results in a spurious-free dynamic range (SFDR) of 89dB in 1MHz resolution bandwidth (RBW).**

***Index Terms*—cognitive radio, cross-correlation, linearity, noise figure, spectrum analyzer, spectrum sensing, spurious-free dynamic range**

I. Introduction

Spectrum sensing is one of the key features that defines cognitive radio (CR) and is an active area of research [1]. A CR-implementation requires a spectrum analyzer (SA) of some form to find unoccupied bandwidth (white spots). However, not all white spots are identical in terms of receiver requirements. It is shown in [2] that, depending on the spectral location of strong signals, each white spot poses different linearity requirements, some of which cannot be met with current state-of-the-art receivers. Spectral sensing in combination with some digital signal processing (DSP) can therefore be vital to choose a white spot with relaxed receiver requirements, i.e., to avoid spots where IM3 distortion occurs [2], [3].

Currently, the Federal Communications Commission (FCC) requires geolocation in combination with spectrum sensing for CR in the TV-bands. It considers stand-alone use of spectrum sensing to be too unreliable, because industrial prototypes failed to detect weak signals in the presence of a large interferer [4]. It is likely that this inability of the prototypes is due to their limited spurious-free dynamic range (SFDR), which will be explained further on.

For commercial CR applications, it is desirable to have a low-cost low-power integrated solution. Because CRs will also require a fair share of DSP, complementary Metal-Oxide-Semiconductor (CMOS)-technology seems like the ideal candidate. However, CMOS has its limitations, especially in terms of linearity due to the low supply voltage.

In this paper we will improve both linearity and noise of a CMOS-receiver, and hence SFDR, by using two identical radio frequency (RF) front-ends in combination with attenuators and cross-correlation. We will show that, compared to the single RF front-end [5], we can achieve a 13 dB higher input-referred third-order intermodulation intercept point (IIP3) and a 2 dB lower noise figure (NF), increasing SFDR by 10 dB.

The remainder of this paper is organized as follows: section II will discuss SFDR in more detail, while section III explains the basic principle of cross-correlation. Section IV covers the implementation aspects of the cross-correlation SA, followed by measurement results in section V. Conclusions are drawn in section VI.

II. Spurious-Free Dynamic Range

The SFDR is an important parameter of a SA and defines the difference in decibels between the strongest and weakest signal that can be detected *at the same time* [6].[1] It is important for CR-applications in the TV-bands (47–700 MHz) because of the huge dynamic range of received signals. The SFDR is limited by non-linearity and noise [7].

To understand the effects of non-linearity, the analog front-end is modeled as a weakly nonlinear system, which in the time domain can be represented as

$$s_{\text{out}} = \alpha_1 s_{\text{in}} + \alpha_2 s_{\text{in}}^2 + \alpha_3 s_{\text{in}}^3 + \dots \quad (1)$$

where s_{in} is the input signal (usually in Volt), s_{out} is the output signal of the system and α_i are constant factors depending on the design of the front-end. The even-order distortion products are canceled to a high degree with a differential implementation. In practice, $\alpha_3 s_{\text{in}}^3$ is the most important remaining distortion-introducing term. The distortion introduced by this term can be quantified using IIP3 [7]. Assume two sinusoids, at frequencies f_1 and f_2 and each with power P, are applied to the input of the system. IIP3 is defined to be P when the power of the distortion component $(2f_1 - f_2)$ at the output caused by $\alpha_3 s_{\text{in}}^3$ is equal to the power of a desired component (f_1 or f_2) at the output. IIP3 is usually found by extrapolation, because at high input powers the weak nonlinearity approximation of eq. (1) is not valid anymore.

[1] Definitions of SFDR differ between fields and even authors in the same field. We have assumed the definition as used for the SFDR in SA-datasheets.

978-1-4244-5188-3/10/$26.00 ©2010 IEEE

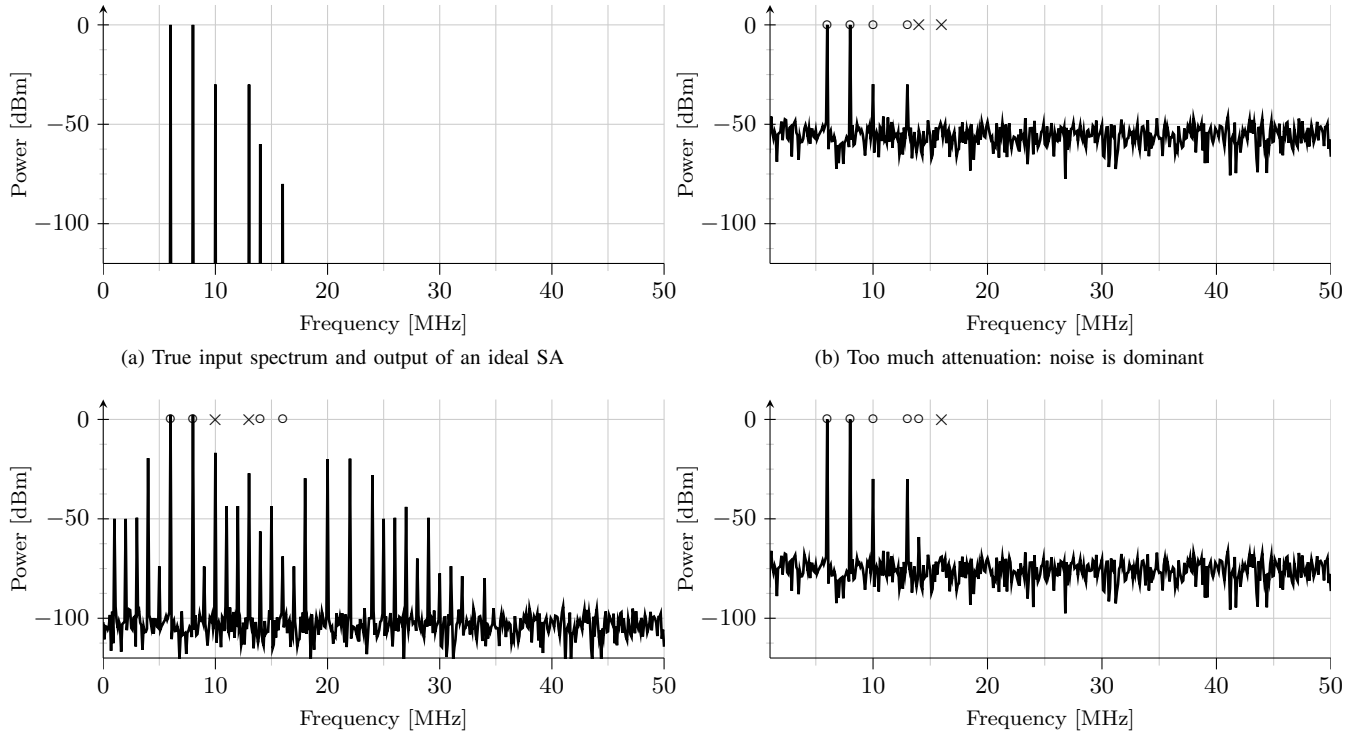

(a) True input spectrum and output of an ideal SA

(b) Too much attenuation: noise is dominant

(c) Not enough attenuation: non-linearity is dominant

(d) Optimum setting of attenuation: noise and non-linearity equally dominant

Fig. 1: Simulation of a SA (NF=20 dB, IIP3=+10 dBm) with RBW=100 kHz. Because of the limited SFDR it is not possible to detect all input signals at the same time. The ∘-symbol indicates detection of the signal, × indicates that the signal is obscured by distortion products or noise, and peaks without a symbol are pure distortion components.

An attenuation of x dB requires s_{in} to have x dB more power to introduce the same distortion at the output, and hence IIP3 is increased by x dB. A passive attenuator with x dB loss in front of a receiver degrades NF by x dB. In total, passive attenuation of x dB at the input increases both NF and IIP3 by x dB [7].

The following equation for SFDR can be derived (which is valid if the SFDR is limited by NF and IIP3) [6], [7]

$$\text{SFDR} = \frac{2}{3}\left(\text{IIP3} - \text{NF} - 10\log_{10} B + 174\right) \text{ [dB]} \quad (2)$$

where B is the resolution bandwidth (RBW).

The effect of a limited SFDR is shown in fig. 1 for a simulated SA with NF=20 dB and IIP3=+10 dBm ($\alpha_1 = 1$ and $\alpha_3 = 8/3$ V^{-2}) using a RBW of 100 kHz. The measured spectrum (in this case: simulation) deviates from the true spectrum due to noise and non-linearity. If the signal is not attenuated enough, distortion components limit the ability to detect weaker signals.[2] On the other hand, if the signal is attenuated too much, noise limits this ability. The SFDR of 76 dB is obtained *only at an optimum setting of the attenuation*, but even then not all signals can be detected. Many SAs provide an adjustable attenuator to achieve the optimum setting.

State-of-the-art CMOS-receivers typically achieve an IIP3 of −10 dBm to 0 dBm and a NF of 5 dB to 8 dB, resulting in a maximum SFDR of around 70 dB in a RBW of 1 MHz. A trade-off in receiver design can be made: adding a low-noise amplifier (LNA) in front of a noisy mixer leads to a better NF, but reduces linearity. Hence, the goal to achieve a higher SFDR is not reached.

[2]Note that attenuation is digitally corrected for, as is done in all SAs, because knowledge of the true input power of the signal is desired.

III. Cross-correlation

Any practical system adds noise to the signal to be processed. In a traditional SA, a form of autocorrelation (energy detection) is performed, where the front-end adds noise n to the signal a, which results in the power spectral density (PSD) of $a + n$ [8], see fig. 2a. If n is large compared to a, a will be obscured by the noise.

Using cross-correlation, two independent front-ends add noise n_1 and n_2 respectively, giving signals $u = a + n_1$ and $v = a + n_2$. The resulting cross-spectrum $P_{uv} = P_{aa} + P_{an_2} + P_{n_1 a} + P_{n_1 n_2}$ converges to P_{aa} for increasing integration time, because the other terms have an expected value of 0 when the signal and the noise sources are uncorrelated. The cross-correlation SA is schematically shown in fig. 2b.

It can be shown that the effective noise power added by the system decreases with 1.5 dB for every doubling of measurement time [9]–[11], and can be reduced by as much as 50 dB [9].

Using cross-correlation to lower system noise is not a new idea; it is in widespread use in radio-astronomy [12], it has

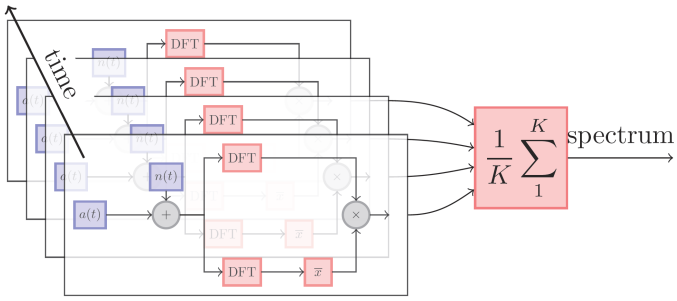

(a) Autocorrelation SA

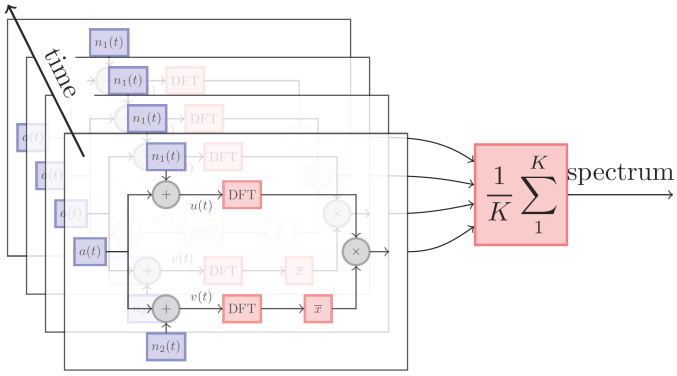

(b) Cross-correlation SA

Fig. 2: Schematic representation of a traditional SA (autocorrelation, with averaging to smoothen the noise floor) and our cross-correlation SA. $\overline{x}$ denotes complex conjugation.

been used in [9] to measure the thermal noise of a resistor, and it is briefly mentioned in [13] as more robust in the presence of noise uncertainty. In communications literature the content seems to be limited. In [11], cross-correlation is discussed (but not implemented) in terms of noise performance, where it is concluded that it "may provide a viable way to relieve the requirement of the analog part of the spectrum sensing receiver." Cross-correlation was proposed in [14] to mitigate the effects of harmonic downmixing on spectrum sensing, but the paper does not address noise and linearity issues. We assume that harmonic downmixing in our SA is not the key problem, as it can be reduced by external RF-filters and/or the technique of [14], and focus on linearity and SFDR.

After long-enough correlation time, only a negligible amount of uncorrelated system noise will be left. At this point, cross-correlation behaves as autocorrelation: only the correlated part of noise sources n_1 and n_2 in fig. 2b remains, reducing the system to fig. 2a.

It is well known for energy detection that even the slightest amount of uncertainty in the noise level leads to an SNR wall: a minimum SNR below which reliable sensing becomes impossible, even with infinite measurement time [15]–[17]. When at least part of n_1 and n_2 is uncorrelated, the NF of the system is reduced after cross-correlation, which is equivalent to an improvement in SNR. Therefore, with an SNR wall set by noise uncertainty, the absolute signal power that can be detected is improved. In other words, cross-correlation has

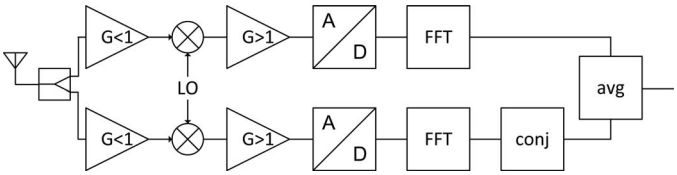

Fig. 3: Block diagram of the cross-correlation system.

a better sensitivity than autocorrelation. Cross-correlation is also more robust against gain variations and other analog imperfections [12]. These advantages come at the cost of duplication of the front-end and a slight increase in digital processing.

Apart from the aforementioned differences, cross-correlation shares all properties with autocorrelation. This means that all comparisons between detectors, such as [1], [15], [16], can still be used, while keeping in mind the improved sensitivity of cross-correlation.

Spectrum sensing techniques capable of extracting signals far below the noise floor are usually computationally intensive and require knowledge of the signals to be detected. Requiring knowledge of the signal to be detected is undesired, because the concept of CR applies to any frequency band, where each band may contain a myriad of different modulation techniques. Due to the SNR wall of energy detection, it is not unlikely that specialized algorithms will still be required in some cases to obtain the desired sensitivity. Therefore, energy detection could be used as a first general method to scan the spectrum and already discard as many occupied bands as possible. As cross-correlation is a more robust way of energy detection than traditional autocorrelation, it allows specialized algorithms to concentrate on fewer candidate bands.

IV. Implementation

As cross-correlation reduces noise only by 1.5 dB per doubling of measurement time, the system should preferably already have a good SFDR before cross-correlation. Therefore, we use an LNA-less receiver concept [5], which is already highly linear (IIP3=+11 dBm) and low-noise (NF<6.5 dB). A block diagram of the cross-correlation system is shown in fig. 3.

The system assumes a differential input signal, and uses passive power splitters to connect the input to the two front-ends. A resistor network in front of the front-ends provides impedance matching and attenuates the signal, after which it is downconverted and filtered by the on-chip mixer [5]. The differential I- and Q-signals are first amplified on-chip by IF-amplifiers, and again amplified off-chip by opamps to properly interface with the 14-bit analog-to-digital converters (ADCs). For this experiment, the digital processing is performed on a PC using double floating-point precision. Our prototype contains external resistors, while the RF-frontend is integrated in 65nm CMOS [5], see fig. 4. Note that it is very well possible to integrate the external resistors, the off-chip amplifiers, the ADCs and the DSP with the RF front-ends on one CMOS-chip.

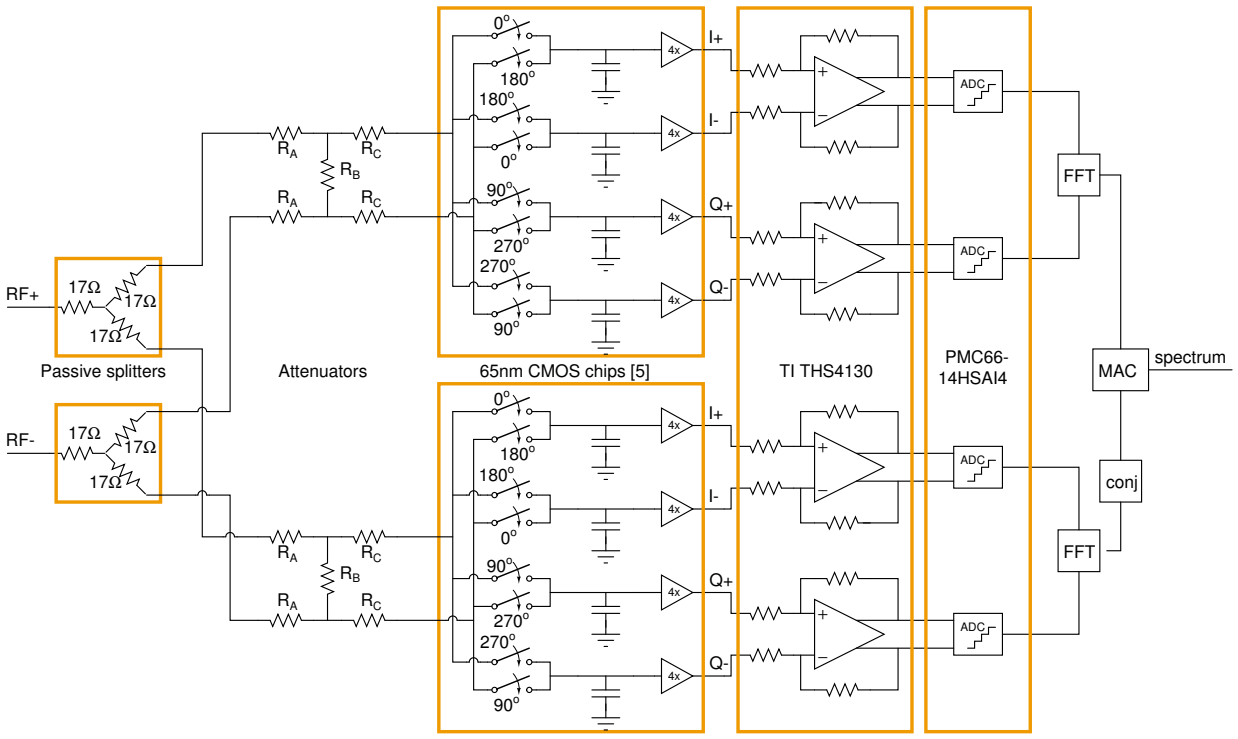

Fig. 4: Implementation of our cross-correlation system

In order to realize $50\,\Omega$-matching (to allow for the use of standard $50\,\Omega$ RF pre-filters to reduce interference and harmonic downmixing), we use an H-network of resistors in front of the mixer (see fig. 4). Using different values for R_A, R_B and R_C, a step-attenuator can be implemented to increase linearity at the cost of noise. The resistor values can be calculated based on the input impedance of the mixer at the mixing frequency, which is derived in [18]. Cross-correlation can then be used to lower the increased noise, while leaving the increased linearity intact, resulting in a higher SFDR.

We used two networks for measurements, see fig. 5. Network 1 provides plain matching (which is $100\,\Omega$ because the circuit is differential). Because the mixers are voltage-sensing devices with a high input impedance, the signal is already attenuated by 6 dB as compared to the setup in [5]. Network 2 adds another 6 dB of attenuation. The choice was based on obtaining a considerable improvement in linearity, while not increasing integration time too much for NF measurements or practical applicability.

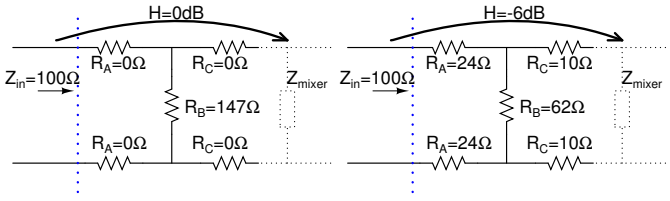

(a) Network 1: plain matching (b) Network 2: 6 dB attenuation

Fig. 5: The two attenuation networks used for measurements.

V. Measurements

Figure 6 shows measurement results of the NF as a function of measurement time for different RF-frequencies and different attenuation networks. A normalized measurement time (NMT) of 1 is defined as the minimum time necessary for a single spectral estimate under the same conditions (RBW, sample rate) as used for autocorrelation.

When uncorrelated system noise is dominating over source noise and correlated system noise, the NF decreases by 1.5 dB/octave, as expected. Some residual noise floor can be observed, part of which probably originates from noise-folding of the mixer and aliasing of the ADCs of the source noise, which is correlated in both front-ends. We observed that parasitic coupling between the front-ends can also lead to correlated noise. One can also clearly observe the 6 dB difference in NF between the two attenuation networks. The small difference in NF between different RF-frequencies using the same attenuation network is attributed to the measurement setup.

When using the front-end with network 2, ADCs sampling at 10 MS/s, and a RBW of 1 MHz, obtaining enough samples for each fast Fourier transform (FFT) takes $0.1\,\mu$s. From fig. 6, the effective NF decreases from 24 dB to 10 dB after 800 FFTs, which takes only $80\,\mu$s. For CR this increase in measurement time can be acceptable.

Figure 7 shows measured spectra for a single cross-correlation measurement at different NMT. The spectra with low NMT look smoother because they have been averaged for

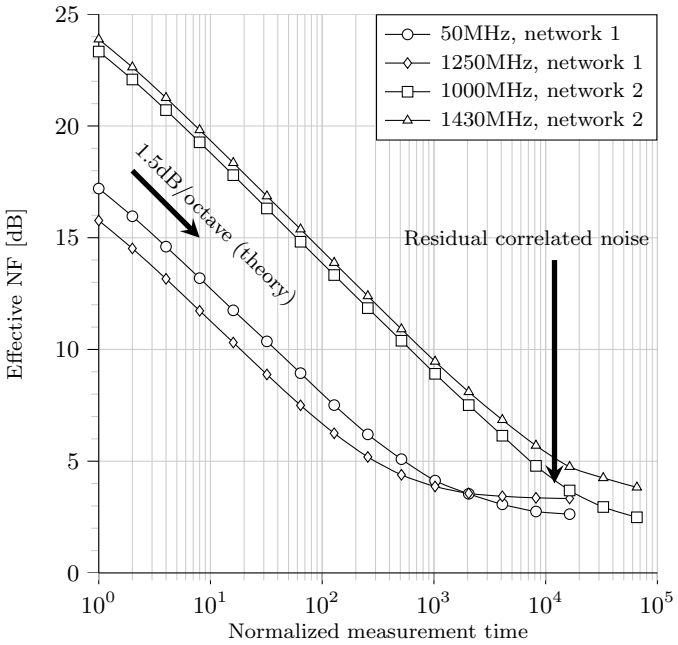

Fig. 6: Measured NF as a function of NMT.

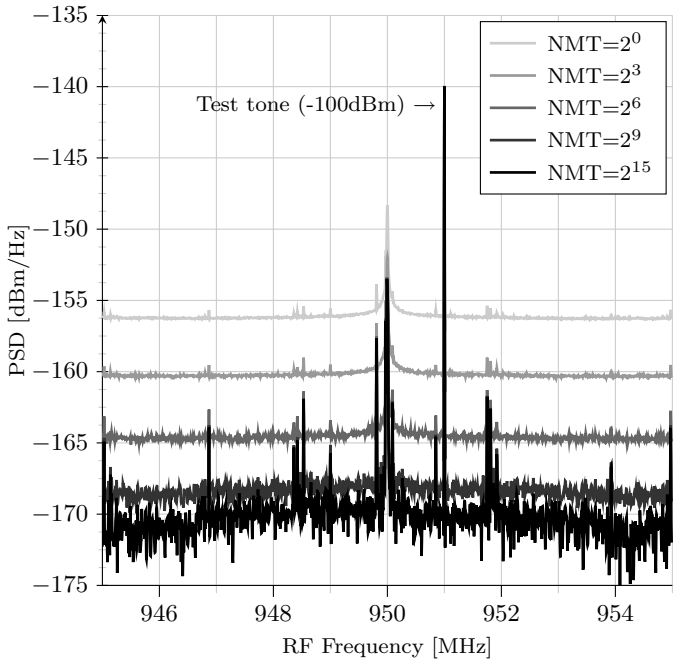

Fig. 7: Measured spectrum as function of correlation time. The test tone of -100 dBm was inserted to verify correct operation. The RBW in this measurement is 10 kHz.

better visibility of the trend in noise reduction. The peak at 950 MHz is caused by DC-offset of our zero-IF front-end.

Measurement results for NF and IIP3 over the whole bandwidth of operation are shown in fig. 8. It can be clearly seen that the additional 6 dB of attenuation increases both NF and IIP3 by 6 dB, but the additional NF is completely reduced by cross-correlation. As a result, using eq. (2), the SFDR

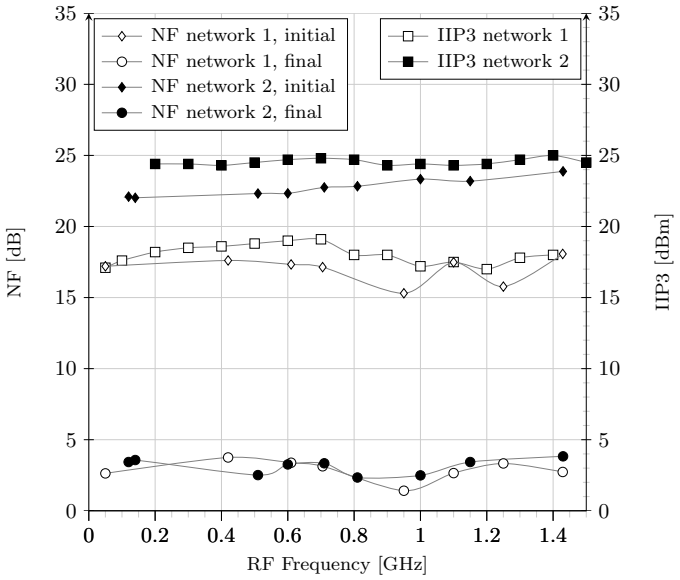

Fig. 8: NF and IIP3 measurement results

is increased by 4 dB. For both attenuation networks, the NF after cross-correlation is lower than for the original front-end without attenuator. For network 2, the SFDR is increased by 10 dB as compared to the single front-end. The performance of the SA is almost constant over the entire bandwidth of operation.

Each analog front-end (mixer + IF-amplifier) consumes 61 mW ($f_{\mathrm{LO}} = 50$ MHz) to 83 mW ($f_{\mathrm{LO}} = 1.5$ GHz). The DSP-part consists of FFTs and multiply-accumulates (MACs). To accommodate the high SFDR of 89 dB in a 1 MHz RBW using fixed-point numbers, we assume 24-bit FFTs (16-bit fixed-point 1024-point FFTs only have a SFDR of 87 dB after cross-correlation) and some additional bits at the accumulators to allow for long integration times. Using the figures of [19] and scaling from 8-bit to 24-bit ($\times 9$), from 2.4 GS/s to 20 MS/s ($\div 120$), from 1 channel to 2 channels ($\times 2$), and allowing 10% more for the MACs, we estimate the DSP power consumption at 25 mW when it is integrated on chip.

Table I compares the results to several other architectures, showing the high linearity and low noise of our design.

VI. Conclusions

Spectrum sensing is a crucial topic for CR. Because very strong and very weak signals can be present at the same time, a SA with a high SFDR is required. The SFDR is limited by noise and non-linearity.

Passive attenuation improves linearity, but degrades noise performance. In this paper it is shown that the degradation in noise performance can be overcome by duplicating a front-end and cross-correlating the outputs of the two front-ends. It relies on the principle that the noise introduced by each front-end is uncorrelated. The noise is reduced at the cost of measurement time: each doubling of measurement time reduces the system-induced noise by 1.5 dB.

TABLE I: Comparison with other designs

Architecture	Technology	RF Freq. [GHz]	Power [mW]	VSWR	NF [dB] [a]	NF [dB] [b]	IIP3 [dBm]	SFDR (RBW=1MHz) [dB]
This work (0,147,0)[c]	65nm CMOS	0.05–1.5	191[d]	< 1.2	17	4	17	85
This work (24,62,10)	65nm CMOS	0.05–1.5	191[d]	< 1.2	23	4	24	89
Soer et al. ISSCC2009 [5]	65nm CMOS	0.2–2.0	67	4.8[e]	6.5	6.5	11	79
Park et al. JSSCC2009 [20]	0.18μm CMOS	0.4–0.9	180	?	50	50	-17[f]	31
Tektronix RSA2203A[g]		0–3		< 1.4	24	24	30	70 / 80[h]
Rohde&Schwarz FSP 3G[g]		0–3		< 2.0	22	22	10	58 / 68[h]
Agilent PSA E4443A[g]		0–7		< 1.6	19	19	16	70 / 74[h]

[a] Minimal measurement time
[b] Maximal measurement time
[c] Meaning $R_A = 0\,\Omega$, $R_B = 147\,\Omega$ and $R_C = 0\,\Omega$
[d] Without ADCs
[e] Calculated at mixing frequency using [18]
[f] P_{1dB} given in paper as -27 dBm
[g] Note that these SAs also contain pre-filters and other components, so the comparison is only indicative
[h] Datasheet / calculated using IIP3 and NF

Through measurements it is shown that the NF can be reduced within acceptable measurement times, making cross-correlation a good candidate for spectral sensing for CR. The achieved IIP3 of $+24$ dBm and NF of 4 dB are 13 dB and 2 dB better, respectively, than what is achieved using a single front-end. In total the SFDR is increased from 79 dB to 89 dB in a 1 MHz RBW. Our performance compares favorably to other designs, as is shown in table I.

By combining cross-correlation with two identical linear front-ends, a high linearity and low NF can be obtained. This allows integrated SAs in CMOS with high SFDR and sensitivity, providing another step towards reliable spectrum sensing for CR.

VII. Acknowledgements

We thank N.A. Moseley, M.J. Bentum, A. Ghaffari and M. Heskamp for many fruitful discussions, G.J.M. Wienk and H. de Vries for the practical assistance and NXP for providing silicon. This research is supported by the Dutch Technology Foundation STW, applied science division of NWO and the Technology Program of the Ministry of Economic Affairs (project 08081).

References

[1] R. Tandra, A. Sahai, and S. M. Mishra, "What is a spectrum hole and what does it take to recognize one?" *Proc. IEEE*, vol. 97, no. 5, pp. 824–848, 2009.

[2] D. H. Mahrof, E. A. M. Klumperink, J. C. Haartsen, and B. Nauta, "On the effect of spectral location of interferers on linearity requirements for wideband cognitive radio front ends," in *Proc. 4th IEEE Symp. on New Frontiers in Dynamic Spectrum Access Networks (DySPAN)*, 2010.

[3] P. F. Marshall, "Dynamic spectrum management of front end linearity and dynamic range," in *Proc. 3rd IEEE Symp. on New Frontiers in Dynamic Spectrum Access Networks (DySPAN)*, 2008, pp. 1–12.

[4] FCC, "In the matter of unlicensed operation in the TV broadcast bands and additional spectrum for unlicensed devices below 900 MHz and in the 3 GHz band," FCC, Tech. Rep., Nov. 2008.

[5] M. C. M. Soer, E. A. M. Klumperink, Z. Ru, F. E. van Vliet, and B. Nauta, "A 0.2-to-2.0GHz 65nm CMOS receiver without LNA achieving >11dBm IIP3 and <6.5 dB NF," in *Proc. IEEE Int. Solid-State Circuits Conf. - Dig. Tech. Papers*, 2009, pp. 222–223,223a.

[6] T. H. Lee, *The Design of CMOS Radio-Frequency Integrated Circuits*. Cambridge University Press, 2004.

[7] C. Rauscher, *Fundamentals of Spectrum Analysis*, 1st ed. Rohde & Schwarz, 2001.

[8] H. Tang, "Some physical layer issues of wide-band cognitive radio systems," in *Proc. 1st IEEE Symp. on New Frontiers in Dynamic Spectrum Access Networks (DySPAN)*, 2005, pp. 151–159.

[9] M. Sampietro, G. Accomando, L. G. Fasoli, G. Ferrari, and E. Gatti, "High sensitivity noise measurement with a correlation spectrum analyzer," *IEEE Trans. Instrum. Meas.*, vol. 49, no. 4, pp. 820–822, Aug. 2000.

[10] J. Briaire and L. K. J. Vandamme, "Uncertainty in gaussian noise generalized for cross-correlation spectra," *J. Appl. Phys.*, vol. 84, pp. 4370–4374, 1998.

[11] M. Heskamp and C. Slump, "Sub-noise primary user detection by cross-correlation," in *Proc. of the Int. Conf. on Communications (ICC)*, Jun. 2009.

[12] A. Thompson, J. Moran, and J. G.W. Swenson, *Interferometry and Synthesis in Radio Astronomy*, 4th ed. Krieger Publishing Company, 1998.

[13] A. Sonnenschein and P. M. Fishman, "Radiometric detection of spread-spectrum signals in noise of uncertain power," *IEEE Trans. Aerosp. Electron. Syst.*, vol. 28, no. 3, pp. 654–660, 1992.

[14] N. A. Moseley, E. A. M. Klumperink, and B. Nauta, "A spectrum sensing technique for cognitive radios in the presence of harmonic images," in *Proc. 3rd IEEE Symp. on New Frontiers in Dynamic Spectrum Access Networks (DySPAN)*, 2008, pp. 1–10.

[15] D. Cabric, A. Tkachenko, and R. W. Brodersen, "Spectrum sensing measurements of pilot, energy, and collaborative detection," in *Proc. IEEE Military Communications Conf. (MILCOM)*, 2006, pp. 1–7.

[16] R. Tandra and A. Sahai, "SNR walls for feature detectors," in *Proc. 2nd IEEE Symp. on New Frontiers in Dynamic Spectrum Access Networks (DySPAN)*, 2007, pp. 559–570.

[17] ——, "Noise calibration, delay coherence and SNR walls for signal detection," in *Proc. 3rd IEEE Symp. on New Frontiers in Dynamic Spectrum Access Networks (DySPAN)*, 2008, pp. 1–11.

[18] B. W. Cook, A. Berny, A. Molnar, S. Lanzisera, and K. S. J. Pister, "Low-power 2.4-GHz transceiver with passive RX front-end and 400-mV supply," *IEEE J. Solid-State Circuits*, vol. 41, no. 12, pp. 2757–2766, 2006.

[19] Y. Chen, Y.-W. Lin, Y.-C. Tsao, and C.-Y. Lee, "A 2.4-Gsample/s DVFS FFT processor for MIMO OFDM communication systems," *IEEE J. Solid-State Circuits*, vol. 43, no. 5, pp. 1260–1273, 2008.

[20] J. Park, T. Song, J. Hur, S. M. Lee, J. Choi, K. Kim, K. Lim, C.-H. Lee, H. Kim, and J. Laskar, "A fully integrated UHF-band CMOS receiver with Multi-Resolution Spectrum Sensing (MRSS) functionality for IEEE 802.22 cognitive radio applications," *IEEE J. Solid-State Circuits*, vol. 44, no. 1, pp. 258–268, 2009.